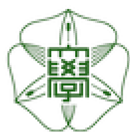
HOKKAIDO UNIVERSITY

Title	Surface Roughness and Magnetic Properties of Ni and Ni78Fe22 Thin Films on Polyethylene Naphthalate Organic Substrates
Author(s)	Kaiju, Hideo; Basheer, Nubla; Kondo, Kenji; Ishibashi, Akira
Citation	IEEE Transactions on Magnetics, 46(6), 1356-1359 https://doi.org/10.1109/TMAG.2010.2045346
Issue Date	2010-06
Doc URL	http://hdl.handle.net/2115/43114
Rights	© 2010 IEEE. Personal use of this material is permitted. However, permission to reprint/republish this material for advertising or promotional purposes or for creating new collective works for resale or redistribution to servers or lists, or to reuse any copyrighted component of this work in other works must be obtained from the IEEE.
Type	article
File Information	TM46-6_1356-1359.pdf

Instructions for use

Hokkaido University Collection of Scholarly and Academic Papers : HUSCAP

Surface Roughness and Magnetic Properties of Ni and $Ni_{78}Fe_{22}$ Thin Films on Polyethylene Naphthalate Organic Substrates

Hideo Kaiju[1,2], Nubla Basheer[1], Kenji Kondo[1], and Akira Ishibashi[1]

[1]Research Institute for Electronic Science, Hokkaido University, Sapporo 001-0020, Japan
[2]PRESTO, Japan Science and Technology Agency, Saitama 332-0012, Japan

We have studied structural, electrical, and magnetic properties of Ni and $Ni_{78}Fe_{22}$ thin films evaporated on polyethylene naphtalate (PEN) organic substrates towards the fabrication of spin quantum cross (SQC) devices. As we have investigated the scaling properties on the surface roughness, the surface roughness of Ni (16 nm)/PEN is 0.34 nm, corresponding to 2 or 3 atomic layers, in the scanning scale of 16 nm, and the surface roughness of $Ni_{78}Fe_{22}$ (14 nm)/PEN is also as small as 0.25 nm, corresponding to less than 2 atomic layers, in the scanning scale of 14 nm. These facts denote that Ni/PEN and $Ni_{78}Fe_{22}/PEN$ are suitable for magnetic electrodes on organic substrates used for SQC devices from the viewpoint of the surface morphology. Then, we have investigated magnetic hysteresis curve and magnetoresistance effects for Ni/PEN and $Ni_{78}Fe_{22}/PEN$. The squareness of the hysteresis loop is as small as 0.24 for Ni (25 nm)/PEN, where there is no observation of the anisotropy magnetoresistance (AMR) effect. In contrast, the squareness of the hysteresis loop is as large as 0.86 for $Ni_{78}Fe_{22}$ (26 nm)/PEN, where the AMR effect has been successfully obtained. These experimental results indicate that $Ni_{78}Fe_{22}/PEN$ is a promising material for use in SQC devices from the viewpoint of not only the surface morphologies but also magnetic properties.

***Index Terms*—Magnetic thin films, polyethylene naphtalate organic substrates, spin quantum cross devices, vacuum evaporation.**

I. INTRODUCTION

MOLECULAR spintronics have extensively attracted interest since the discovery of the magnetoresistance (MR) effect in ferromagnetic metal/organic molecules/ferromagnetic metal [1]–[5]. Xiong *et al.* observed a giant MR effect of 40% at 11 K in $La_{0.67}Sr_{0.33}MnO_3$/tris(8-hydroxy-quinolinato) aluminum (Alq_3)/Co organic spin valve devices [1]. Subsequently, Santos *et al.* obtained a large MR ratio of 7.5% at 4.2 K and 4.6% at room temperature in $Co/Al_2O_3/Alq_3$/NiFe magnetic tunnel junctions [2]. Moreover, many researchers have confirmed a large MR effect in $La_{0.7}Sr_{0.3}MnO_3/Alq_3/Al_2O_3/Co$ [3], Co/4,4′-bis99-(ethyl-3-carbazovinylene)-1,1′- biphenyl (CVB)/$La_{0.67}Sr_{0.33}MnO_3$ [4], and $La_{0.67}Sr_{0.33}MnO_3$/tetraphenyl porphyrin(TPP)/Co [5]. Recently we have proposed spin quantum cross (SQC) devices, in which organic molecules are sandwiched between two edges of magnetic thin films deposited on organic substrates with their edges crossing [6], [7]. A schematic of the fabrication procedure of SQC devices has been reported in our previous paper [6]. In SQC devices, the junction area can be scaled down to dimensions of a few nanometers because the thickness of magnetic thin films is determined by the growth rate, ranging from 0.01 to 1.0 nm/s, if there is no pinhole, diffusion and penetration into organic layers. According to our recent calculation performed within the framework of the Anderson model, SQC devices exhibit a giant MR effect at room temperature [8]. In this paper, towards the fabrication of SQC devices, we have investigated structural, electrical, and magnetic properties of Ni and $Ni_{78}Fe_{22}$ thin films evaporated on polyethylene naphtalate (PEN) organic substrates and discussed their feasibility for use in SQC devices.

Manuscript received October 25, 2009; revised January 29, 2010; accepted March 05, 2010. Current version published May 19, 2010. Corresponding author: H. Kaiju (e-mail: kaiju@es.hokudai.ac.jp).

Color versions of one or more of the figures in this paper are available online at http://ieeexplore.ieee.org.

Digital Object Identifier 10.1109/TMAG.2010.2045346

II. EXPERIMENTS

Ni and $Ni_{78}Fe_{22}$ thin films were thermally evaporated on PEN substrates (5 mm width, 4 mm length, 20 μm thickness) under a magnetic field of 30 kA/m in a high vacuum chamber at a base pressure of $\sim 10^{-8}$ torr. PEN films TEONEX Q65 were supplied by Teijin DuPont Japan. A boron nitride crucible $N-1$, made by DENKA, and a tungsten filament, made by CRAFT, were used for the thermal evaporation of Ni and $Ni_{78}Fe_{22}$ thin films. A heat-block stainless plate with a hole was inserted between the Ni and $Ni_{78}Fe_{22}$ vapor source and the PEN substrate. The length of the crucible and the aperture size in the stainless plate were designed using a geometrical simulation to evaporate uniform Ni and $Ni_{78}Fe_{22}$ films in-plane to PEN substrates. The temperature near PEN substrates was less than 62 °C, which was lower than the glass transition temperature T_g of 120 °C for PEN substrates. The pressure during the evaporation was 10^{-5} torr and the growth rate was 0.93 nm/min at an evaporation power of 350 W. The Ni and $Ni_{78}Fe_{22}$ thicknesses were measured by a mechanical method using the stylus surface profiler DEKTAK and an optical method using a He-Ne laser at a wavelength of 632.8 nm and a photo diode detector. The surface morphologies of samples were analyzed by an atomic force microscope (AFM) Nanoscope IIIa. The analysis of the surface roughness, based on AFM images, was performed by the image analysis software Gwyddion. The magnetization curve was measured by a superconducting quantum interference device (SQUID) magnetometer MPMS-XL at room temperature under a magnetic field up to 1 T. The MR curve was measured using dc four-probe method with a constant current of 1 mA and a magnetic field up to 0.3 T at room temperature.

III. RESULTS AND DISCUSSION

Fig. 1 shows the 3-D surface images obtained from AFM observation for: a) PEN; b2) Ni (16 nm)/PEN; c) $Ni_{78}Fe_{22}$

Authorized licensed use limited to: HOKKAIDO DAIGAKU KOHGAKUBU. Downloaded on June 14,2010 at 07:01:59 UTC from IEEE Xplore. Restrictions apply.

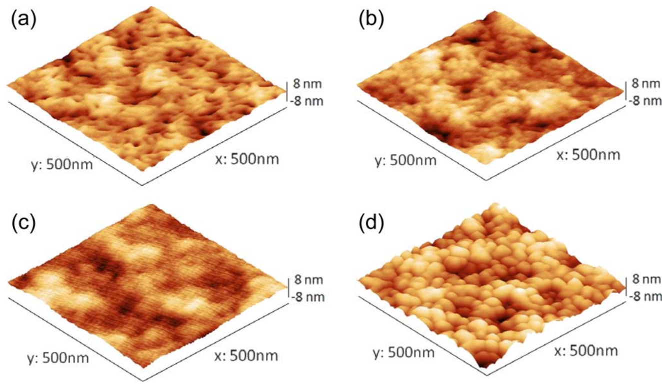

Fig. 1. Surface morphology of (a) PEN, (b) Ni (16 nm)/PEN, (c) $Ni_{78}Fe_{22}$ (14 nm)/PEN, and (d) Au (14 nm)/PEN.

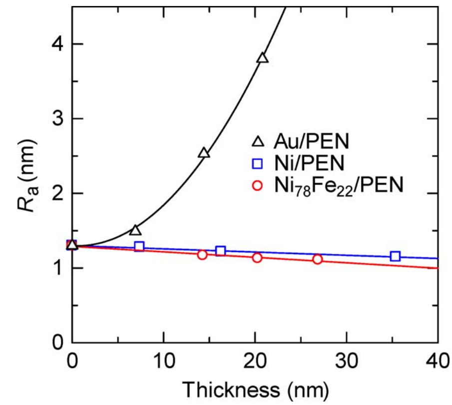

Fig. 2. Surface roughness as a function of the metal film thickness for Ni/PEN, $Ni_{78}Fe_{22}/PEN$, and Au/PEN.

(14 nm)/PEN; and d) Au (14 nm)/PEN. From the 3-D images, which are 500 nm $\times$ 500 nm in area, mound-like surfaces are observed in Ni (16 nm)/PEN, $Ni_{78}Fe_{22}$ (14 nm)/PEN, and Au (14 nm)/PEN, and are classified by the surface roughness. Here, the surface roughness (R_a) is defined by

$$R_a = \frac{1}{L_x L_y} \int_0^{L_x} \int_0^{L_y} |h(x,y)|\, dxdy \tag{1}$$

where $h(x,y)$ is the height profile as a function of x and y and $L_{x(y)}$ is the lateral scanning size in the $x(y)$ direction. R_a of PEN is 1.3 nm, which is smaller than widely-used organic films, such as polyethylene terephthalate (PET) and polyimide. R_a's of Ni (16 nm)/PEN and $Ni_{78}Fe_{22}(14\ nm)/PEN$ are also as small as 1.22 and 1.17 nm, respectively. In contrast, R_a is as large as 2.53 nm for Au (14 nm)/PEN. Fig. 2 shows R_a as a function of the metal film thickness for Ni/PEN, $Ni_{78}Fe_{22}/PEN$, and Au/PEN. R_a increases up to 3.8 nm for a film thickness of 21 nm for Au/PEN. In comparison, R_a decreases slightly down to 1.1 and 1.0 nm with increasing the film thickness for Ni/PEN and $Ni_{78}Fe_{22}/PEN$, respectively. Here, we consider the growth mode of Ni/PEN and $Ni_{78}Fe_{22}/PEN$, and discuss their feasibility in SQC devices from the viewpoint of the surface roughness. Fig. 3 shows the scaling properties of R_a for PEN, Ni/PEN, and $Ni_{78}Fe_{22}/PEN$. The inset represents the scaling properties of the root mean square (RMS) surface roughness (R_q). R_q obeys a scaling law, $R_q = w(L) \propto L^{\alpha}$, where $w(L)$ is the interface width corresponding to the standard deviation of the surface height, L is the system size, and α is the growth scaling exponent. The growth scaling exponent for roughening $w(L) \propto L^{\alpha}$ has been widely used to characterize the growth of a solid from a vapor, such as the epitaxial growth of Fe/Si (111) [9], growth of evaporated Ag/quartz [10], and molecular beam epitaxial growth of $CuCl/CaF_2(111)$ [11], as described by the Kardar-Parisi-Zhang (KPZ) equation [12]. As for PEN, Ni/PEN, and $Ni_{78}Fe_{22}/PEN$, α shows the almost constant value of 0.64-0.68, as seen from the similar roughness slope in any sample. This indicates that the surface morphology of Ni/PEN and $Ni_{78}Fe_{22}/PEN$ exhibits almost the same behavior as that of PEN and these results are consistent with the 3-D AFM observation in Fig. 1. We have also found that the surface is described as self-affine due to $\alpha \neq \beta$, where β is the dynamical exponent in a scaling law $R_q = w(t) \propto t^{\beta}$. Here, t is a growth thickness. As one can see from Fig. 2, β is the negative value since the surface roughness slightly decreases with increasing the thickness for Ni/PEN and $Ni_{78}Fe_{22}/PEN$. This results in $\alpha \neq \beta$, which shows the self-affine growth and it can also be seen in sputtered copper films [13] and evaporated silver films on silicon substrates [14]. The growth process itself of Ni and $Ni_{78}Fe_{22}$ thin films on PEN organic substrates is of great interest and is rich in physics, so detailed work including the dynamic physical mechanism, such as the random deposition and ballistic deposition, will be reported elsewhere. Here, we consider their feasibility in SQC devices from the viewpoint of the surface roughness. Since the junction area in SQC devices is determined by the film thickness, we need to clarify the surface roughness in the same scanning scale as the thickness size. As shown in Fig. 3, R_a of Ni (16 nm)/PEN is 0.34 nm, corresponding to 2 or 3 atomic layers, in the scanning scale of 16 nm. The surface roughness of $Ni_{78}Fe_{22}(14\ nm)/PEN$ is also as small as 0.25 nm, corresponding to less than 2 atomic layers, in the scanning scale of 14 nm. These results denote that the number of molecules sandwiched between two magnetic thin films in SQC devices can be strictly determined in a high resolution of 1-3 atoms by controlling the thickness of Ni and $Ni_{78}Fe_{22}$ thin films and it leads to a high product yield of magnetic head devices and magnetic sensors due to the reduction of the fluctuation in a junction resistance. These facts indicate that Ni/PEN and $Ni_{78}Fe_{22}/PEN$ are suitable for magnetic metal thin films on organic substrates used for SQC devices from the viewpoint of the surface morphology.

Finally, we discussed their feasibility in SQC devices from the viewpoint of the magnetic properties. Fig. 4 shows the magnetization curve and the MR effect for Ni (25 nm)/PEN and $Ni_{78}Fe_{22}(26\ nm)/PEN$. These experiments have been carried out at room temperature. In Fig. 4(a) and (c), the magnetic field is applied in the same direction as the in-plane magnetic field applied during the evaporation. This direction is expected as the easy-axis direction since the Ni and $Ni_{78}Fe_{22}$ films have polycrystalline structures. From Fig. 4(a), the squareness of the hysteresis loop M_r/M_s is as small as 0.24 for Ni (25 nm)/PEN. Here, M_r and M_s are the residual and saturation magnetization, respectively. This low squareness means that the uniaxial

Authorized licensed use limited to: HOKKAIDO DAIGAKU KOHGAKUBU. Downloaded on June 14,2010 at 07:01:59 UTC from IEEE Xplore. Restrictions apply.

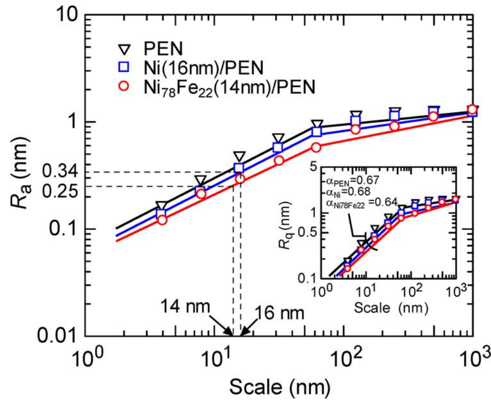

Fig. 3. Scaling properties of the surface roughness $R_{\rm a}$ for PEN, Ni(16 nm)/PEN and $\rm Ni_{78}Fe_{22}$ (14 nm)/PEN. The inset shows scaling properties of the RMS surface roughness $R_{\rm q}$. The solid lines represent fitting lines. The slight difference of the solid lines between the main figure and the inset is due to the difference of the definition for $R_{\rm a}$ and $R_{\rm q}$.

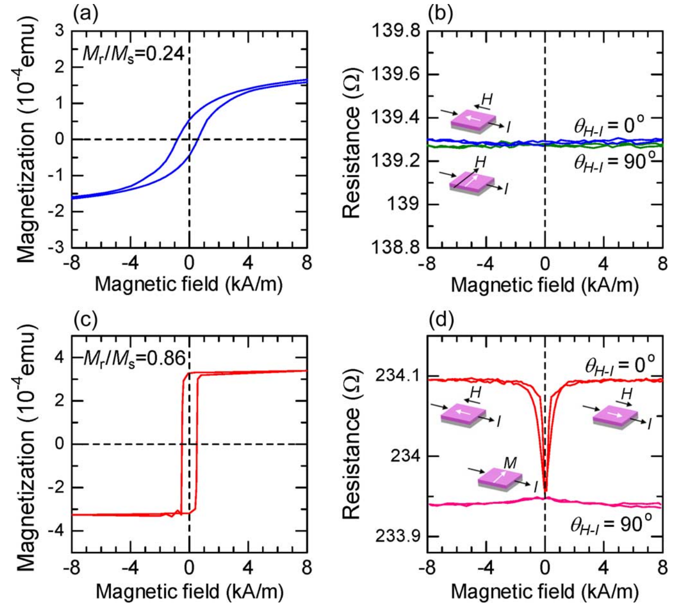

Fig. 4. (a) Magnetization curve and (b) magnetoresistance effect for Ni (25 nm)/PEN and (c) magnetization curve and (d) magnetoresistance effect for $\rm Ni_{78}Fe_{22}$ (26 nm)/PEN at room temperature.

magnetic anisotropy cannot be induced. Fig. 4(b) shows the MR curve for Ni (25 nm)/PEN. The magnetic field is applied parallel to the current $(\theta_{H-I}=0^{\circ})$ and is applied perpendicular to the current $(\theta_{H-I}=90^{\circ})$. Since the Ni films are smooth as shown in Fig. 2, they should provide an anisotropy magnetoresistance (AMR) effect. However, the AMR effect has not been observed. Ni (17 nm)/PEN and Ni (39 nm)/PEN also provide no AMR effect. At the present stage, the reason is not clear. Further experiments and analyses will be required in near future. In contrast, from Fig. 4(c), the squareness of the hysteresis loop is as large as 0.86 for $\rm Ni_{78}Fe_{22}(26\ nm)/PEN$. This high squareness means that the uniaxial magnetic anisotropy can be induced. This indicates that $\rm Ni_{78}Fe_{22}/PEN$ is suitable for SQC devices due to large dM/dH, which is related to the sensitivity in magnetic signal for magnetic head devices and magnetic sensors. Fig. 4(d) shows the MR curve for $\rm Ni_{78}Fe_{22}(26\ nm)/PEN$. The magnetic field is applied in the same direction as shown in Fig. 4(b). The AMR effect can be observed for $\rm Ni_{78}Fe_{22}(26\ nm)/PEN$ although it cannot be observed for Ni/PEN. The minimum value of the resistance measured in the hard-axis direction $(\theta_{H-I}=0^{\circ})$ is almost the same as the resistance measured in easy-axis direction $(\theta_{H-I}=90^{\circ})$. This means that the magnetization at 0 Oe is aligned perpendicular to the current when the magnetic field is applied in the hard-axis direction $(\theta_{H-I}=0^{\circ})$. However, the AMR ratio is as small as 0.07%, which is smaller than the typical value of 1%-2% observed in NiFe thin films [15], [16]. The AMR ratios for $\rm Ni_{78}Fe_{22}(16\ nm)/PEN$ and $\rm Ni_{78}Fe_{22}(43\ nm)/PEN$ are also as small as 0.05% and 0.11%, respectively. The reason why the AMR ratio is small is due to a high resistivity ρ of 300-800 $\mu\Omega$cm for $\rm Ni_{78}Fe_{22}/PEN$. In the case of $\rm Ni_{78}Fe_{22}(26\ nm)/PEN$, ρ is 760 $\mu\Omega$cm, which is much higher than a typical value of 12-32 $\mu\Omega$cm for NiFe thin films [15]. If ρ is around 32 $\mu\Omega$cm for $\rm Ni_{78}Fe_{22}(26\ nm)/PEN$, the AMR ratio can reach up to 1.7%. Actually, the resistivity change $\Delta\rho$ for $\rm Ni_{78}Fe_{22}(26\ nm)/PEN$ is 0.49 $\mu\Omega$cm, which is almost the same as a reported value of 0.50-0.64 $\mu\Omega$cm for NiFe thin films [15]. Therefore, in order to improve the AMR ratio, the reduction of ρ is necessary. Thus, although the AMR signal is small in our experiments and the improvement of the AMR ratio is required, the presence of the AMR effect and the sharp slope of dM/dH for $\rm Ni_{78}Fe_{22}/PEN$ are of great importance. These experimental results indicate that $\rm Ni_{78}Fe_{22}/PEN$ is a good candidate for use in SQC devices from the viewpoint of not only the surface morphologies but also magnetic properties, and can also be expected for potential application in novel devices such as flexible magnetic sensors.

ACKNOWLEDGMENT

This work was supported in part by Special Education and Research Expenses from Post-Silicon Materials and Devices Research Alliance, a Grant-in-Aid for Young Scientists from The Ministry of Education, Culture, Sports, Science, and Technology (MEXT), Precursory Research for Embryonic Science and Technology Program and Research for Promoting Technological Seeds from Japan Science and Technology Agency (JST), Foundation Advanced Technology Institute (ATI), and a Grant-in-Aid for Scientific Research from Japan Society for the Promotion of Science (JSPS). The authors would like to thank Dr. M. Hirasaka of Teijin Ltd., Research Manager K. Kubo of Teijin DuPont Films Japan Ltd., Associate Prof. M. Ishimaru of Osaka University, Prof. M. Yamamoto, Assistant Prof. K. Matsuda, Associate Prof. T. Akutagawa, Assistant Prof. S. Noro, Dr. S. Jin, H. Sato, and M. Takei of Hokkaido University for their helpful discussions.

REFERENCES

[1] Z. H. Xiong, D. Wu, Z. V. Vardeny, and J. Shi, "Giant magnetoresistance in organic spin-valves," *Nature*, vol. 427, pp. 821–824, Feb. 2004.
[2] T. S. Santos, J. S. Lee, P. Migdal, I. C. Lekshmi, B. Satpati, and J. S. Moodera, "Room-temperature tunnel magnetoresistance and spin-polarized tunnelling through an organic semiconductor barrier," *Phys. Rev. Lett.*, vol. 98, pp. 0166011–0166014, Jan. 2007.
[3] V. Dediu, L. E. Hueso, I. Bergenti, A. Riminucci, F. Borgatti, P. Graziosi, C. Newby, F. Casoli, M. P. De Jong, C. Taliani, and Y. Zhan, "Room-temperature spintronic effect in $\rm Alq_3$-based hybrid devices," *Phys. Rev. B*, vol. 78, pp. 1152031–1152036, Sep. 2008.

Authorized licensed use limited to: HOKKAIDO DAIGAKU KOHGAKUBU. Downloaded on June 14,2010 at 07:01:59 UTC from IEEE Xplore. Restrictions apply.

[4] F. J. Wang, C. G. Yang, Z. V. Vardeny, and X. G. Li, "Spin response in organic spin valves based on $La_{2/3}Sr_{1/3}MnO_3$ electrodes," *Phys. Rev. B*, vol. 75, pp. 2453241–2453247, Jun. 2007.

[5] W. Xu, G. J. Szulczewski, P. LeClair, I. Navarrete, R. Schad, G. Miao, H. Guo, and A. Gupta, "Tunneling magnetoresistance observed in $La_{0.67}Sr_{0.33}MnO_3$/organic molecule/Co junctions," *Appl. Phys. Lett.*, vol. 90, pp. 0725061–0725063, Feb. 2007.

[6] H. Kaiju, A. Ono, N. Kawaguchi, and A. Ishibashi, "Surface morphology of gold thin films deposited on polyethylene naphthalate organic films for quantum cross devices," *Japan J. Appl. Phys.*, vol. 47, pp. 244–248, Jan. 2008.

[7] K. Kondo and A. Ishibashi, "Energy spectrum of two-dimensional electron gas to be used quantum cross structures," *Japan J. Appl. Phys.*, vol. 45, pp. 9137–9139, Jan. 2006.

[8] K. Kondo, H. Kaiju, and A. Ishibashi, "Theoretical and experimental results of electronic transport of spin quantum cross structure devices," *J. Appl. Phys.*, vol. 105, pp. 07D5221–07D5223, Apr. 2009.

[9] J. Chevrier, V. Lethanh, R. Buys, and J. Derrien, "A RHEED study of expitaxial-growth of iron on a silicon surface-experimental-evidence for kinetic roughening," *Europhys. Lett.*, vol. 16, pp. 737–742, Oct. 1991.

[10] G. Palasantzas and J. Krim, "Scanning tunneling microscopy study of the thick film limit of kinetic roughening," *Phys. Rev. Lett.*, vol. 73, pp. 3564–3567, Dec. 1994.

[11] W. M. Tong, R. S. Williams, A. Yanase, Y. Segawa, and M. S. Anderson, "Atomic force microscope study of growth kinetics: Scaling in the heteroepitaxy of CuCl on $CaF_2(111)$," *Phys. Rev. Lett.*, vol. 72, pp. 3374–3377, May 1994.

[12] M. Kardar, G. Parisi, and Y.-C. Zhang, "Dynamic scaling growing interfaces," *Phys. Rev. Lett.*, vol. 56, pp. 889–892, Mar. 1986.

[13] K. Ohkawa, T. Nakano, and S. Baba, "Evolution of the scaling of the surface roughness observed on sputtered copper films with atomic force microscope," *J. Vac. Soc. Japan*, vol. 45, pp. 134–137, Mar. 2002.

[14] C. Thompson, G. Palasantzas, Y. P. Feng, S. K. Sinha, and J. Krim, "X-ray-reflectivity study of the growth kinetics of vapor-deposited silver films," *Phys. Rev. B*, vol. 49, pp. 4902–4907, Feb. 1994.

[15] B. Dieny, M. Li, S. H. Liao, C. Horng, and K. Ju, "Effect of interfacial specular electron reflection on the anisotropic magnetoresistance of magnetic thin films," *J. Appl. Phys.*, vol. 88, pp. 4140–4145, Oct. 2000.

[16] R. J. Gambino, M. M. Raja, S. Sampath, and R. Greenlaw, "Plasma-sprayed thick-film anisotropic magnetoresistive (AMR) sensors," *IEEE Sens. J.*, vol. 4, pp. 764–767, Dec. 2004.

Authorized licensed use limited to: HOKKAIDO DAIGAKU KOHGAKUBU. Downloaded on June 14,2010 at 07:01:59 UTC from IEEE Xplore. Restrictions apply.